Robot-Assisted Stereotactic Biopsies in 377 Consecutive Adult Patients with Supratentorial Diffuse Gliomas: Diagnostic Yield, Safety, and Postoperative Outcomes

Marc Zanello[1-3], Alexandre Roux[1-3], Suhan Senova[1,2,4,5], Sophie Peeters[6], Myriam Edjlali[2,3,7], Arnault Tauziede-Espariat[2,8], Edouard Dezamis[1,2], Eduardo Parraga[1,2], Gilles Zah-Bi[1,2], Marc Harislur[1,2], Catherine Oppenheim[2,3,6], Xavier Sauvageon[2,9], Fabrice Chretien[2,8], Bertrand Devaux[1,2], Pascale Varlet[2,3,8], Johan Pallud[1-3]

■ BACKGROUND: **Multiple biopsy samples are warranted for the histomolecular diagnosis of diffuse gliomas in the current molecular era, which possibly increases morbidity.**

■ OBJECTIVE: **We assessed diagnostic yield, safety, and risk factors of postoperative morbidity after robot-assisted serial stereotactic biopsy sampling along 1 biopsy trajectory for diffuse gliomas.**

■ METHODS: **Observational retrospective analysis of consecutive magnetic resonance imaging–based robot-assisted stereotactic biopsies performed at a single institution to assess the diagnosis of nonresectable newly diagnosed supratentorial diffuse gliomas in adults (2006–2016).**

■ RESULTS: **In 377 patients, 4.2 ± 1.9 biopsy samples were obtained at 2.6 ± 1.2 biopsy sites. The histopathologic diagnosis was obtained in 98.7% of cases. Preoperative neurologic deficit ($P = 0.030$), biopsy site hemorrhage ≥20 mm ($P = 0.004$), and increased mass effect on postoperative imaging ($P = 0.014$) were predictors of a new postoperative neurologic deficit (7.7%). Postoperative neurologic deficit ($P < 0.001$) and increased mass effect on postoperative imaging ($P = 0.014$) were predictors of a Karnofsky Performance Status decrease ≥20 points postoperatively (4.0%). Increased intracranial pressure preoperatively ($P = 0.048$) and volume of the contrast-enhanced area ≥13 cm^3 ($P = 0.048$) were predictors of an increased mass effect on postoperative imaging (4.4%). Preoperative Karnofsky Performance Status <70 ($P = 0.045$) and increased mass effect on postoperative imaging ($P < 0.001$) were predictors of mortality 1 month postoperatively (2.9%). Preoperative neurologic deficit ($P = 0.005$), preoperative Karnofsky Performance Status <70 ($P < 0.001$), subventricular zone contact ($P = 0.004$), contrast enhancement ($P = 0.018$), and steroid use ($P = 0.003$), were predictors of the inability to discharge to home postoperatively (37.0%).**

■ CONCLUSIONS: **Robot-assisted stereotactic biopsy sampling results in high diagnostic accuracy with low complication rates. Multiple biopsy sites and samples do not increase postoperative complications.**

INTRODUCTION

Diffuse gliomas in adults are heterogeneous tumors that encompass World Health Organization (WHO) II–IV grades of malignancy.[1,2] Maximal safe surgical resection, if feasible, is recommended as the first-line

Key words
- Glioma
- Neuropathology
- Patient discharge
- Robotic surgical procedures
- Stereotaxic techniques

Abbreviations and Acronyms
FLAIR: Fluid-attenuated inversion recovery
KPS: Karnofsky Performance Status
MRI: Magnetic resonance imaging
WHO: World Health Organization

From the [1]Department of Neurosurgery, GHU site Sainte-Anne, Paris, France; [2]Université de Paris, Paris, France; [3]Institut de Psychiatrie et Neurosciences de Paris (IPNP), INSERM, IMA-BRAIN, Paris, France; [4]Neurosurgery Department, Assistance Publique-Hôpitaux de Paris (APHP), Groupe Henri-Mondor Albert-Chenevier, PePsy department, Créteil, France; [5]INSERM IMR, Université de Paris, Faculté de Médecine, Créteil, France; [6]Department of Neurosurgery, University of California–Los Angeles, Los Angeles, California, USA; and Departments of [7]Neuroradiology, [8]Neuropathology, and [9]Neuro-Anaesthesia and Neuro-Intensive Care, GHU site Sainte-Anne, Paris, France

To whom correspondence should be addressed: Johan Pallud, M.D., Ph.D. [E-mail: johanpallud@hotmail.com; j.pallud@ghu-paris.fr]

Citation: World Neurosurg. (2021) 148:e301-e313.
https://doi.org/10.1016/j.wneu.2020.12.127

*Journal homepage: **www.journals.elsevier.com/world-neurosurgery***

*Available online: **www.sciencedirect.com***

treatment[3] and allows for wide tumor sampling to ascertain the histopathologic diagnosis, to perform additional molecular analyses, and to store samples for future analyses and research.[4-6] If surgical resection is not feasible, a biopsy can be performed. In such cases, ascertaining the histopathologic diagnosis with required molecular analyses is more difficult because of a possible lack of representative tissue sampling and limited tissue material.[7] The risks are grading incorrectly and too low.[5] As a consequence, multiple samples are warranted to increase the likelihood of conclusive diagnosis in the current molecular era, which possibly increases morbidity. Intraoperative histopathologic frozen analysis may be used in addition to ensure the representativity of the biopsy samples.[8]

Robot-assisted stereotactic biopsy allows brain tissue sampling with high precision.[9-11] Since recent pioneering developments, several robotic stereotactic tools have emerged.[12-14] Only a few studies have reported diagnostic yield and safety of robot-assisted stereotactic biopsy[10,11] and have included a small number of patients, the largest cohort being 102 patients.[15-18] A study dedicated to the safety of stereotactic biopsies for the management of diffuse gliomas in the molecular era and using modern tools, such as multimodal magnetic resonance imaging (MRI) guidance and robot assistance, is required. The Sainte-Anne MRI-based robot-assisted stereotactic procedure allows for serial biopsy sampling using MRI to target all components of a diffuse glioma in a single trajectory, in an attempt to obtain an accurate histomolecular diagnosis.[19-22]

The present observational study reports a retrospective consecutive analysis of MRI-based robot-assisted multiple serial stereotactic biopsies performed in our institution to assess the diagnosis of nonresectable diffuse gliomas in adults. We assessed 1) the histomolecular diagnostic yield, 2) the safety of serial stereotactic biopsy sampling along 1 biopsy trajectory, and 3) risk factors of postoperative morbidity, including the number of biopsy samples.

METHODS

Data Source

We reviewed records of adult patients who underwent a stereotactic biopsy for the diagnosis of a cerebral neoplasm at our institution between November 2006 and December 2016 using a protocol designed for the study. Inclusion criteria were 1) patients older than 18 years at the time of surgery; 2) supratentorial tumor location; 3) newly diagnosed WHO grade II, III, or IV diffuse glioma and inconclusive histomolecular diagnosis; and 4) available early postoperative imaging. A patient flowchart is shown in Figure 1.

This study received required authorizations (IRB number 1: 2019/18) of the institutional review board (IRB00011687). The requirement to obtain informed consent was waived for this observational retrospective study according to French legislation.

This study followed the STROBE (Strengthening the Reporting of Observational Studies in Epidemiology) guidelines.[23]

Surgical Procedure

In all patients, robot-assisted serial stereotactic biopsies were performed under general anesthesia according to the updated

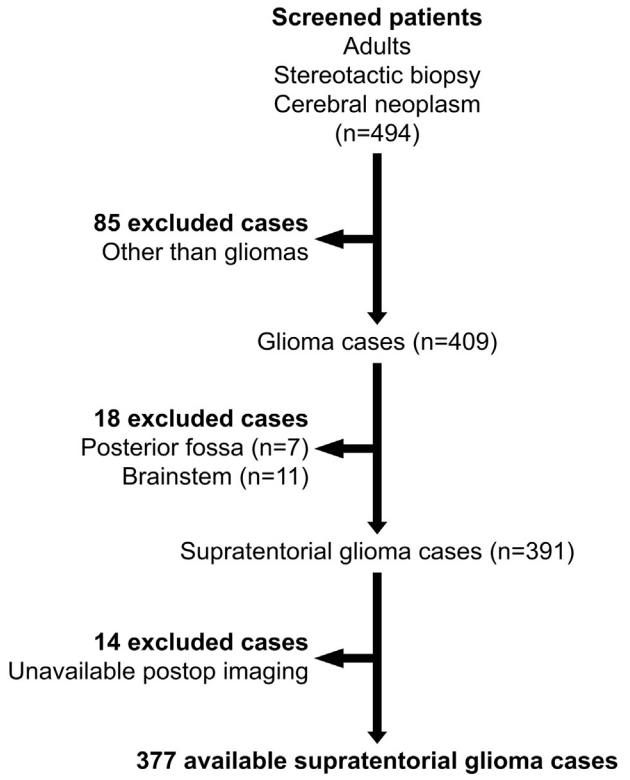

Figure 1. Flowchart showing details of the patient selection process. postop, postoperative.

Sainte-Anne stereotactic method along 1 trajectory to sample all components of the imaging abnormalities.[19,22,24] Preoperative stereotactic MRI (tridimensional T1-weighted sequence with and without contrast agent including midface, acquired in the month before surgery) fused with preoperative oncologic MRI including fluid-attenuated inversion recovery (FLAIR) sequence was used for biopsy trajectory planning and sample selection. The biopsy trajectory was chosen by the neurosurgeon using the iPlanStereotaxy planning software (version 3.0 [BrainLAB AG, Feldkirchen, Germany]) probe's eye view to reach the different tumor components as observed on MRI, avoiding critical structures, such as cerebral sulci, intracranial vessels, and eloquent brain areas. The head of the patient was fixed in a Talairach stereotactic head clamp (Dixi, Besançon, France) fixed to the robot (Neuromate, Renishaw, New Mills, United Kingdom) holder. Biplanar (anteroposterior and lateral) stereoscopic teleangiography radiographs were acquired intraoperatively. The initial biplanar stereoscopic teleangiography radiographs allowed preoperative MRIs to be reformatted in the intraoperative stereotactic space thanks to a fusion between MRIs and these radiographs. Trajectory coordinates were transferred onto the VoXim Neuromate planning software (version 6.0 to version 6.4 [IVS Technology, Germany]). When the arm of the robot was deployed, the entry point and the trajectory were confirmed before drilling of the skull, thanks to biplanar stereoscopic teleangiography radiographs and a metallic punch placed

into the robot tool holder. The biopsy cannula was introduced manually under the guidance of the robotic arm following the defined trajectory through a drill hole made with a 2.5-mm-diameter drill bit. Biopsy cannula movements were then controlled by the robot, ensuring accurate positioning at each biopsy site. Biopsy samples were obtained using a 10-mm window side-cutting Sedan-Vallicioni biopsy cannula. Biplanar stereoscopic teleradiographic radiographic images were taken at each biopsy site before collecting the samples to verify the position of the cannula. Typically, the first biopsy sampling site was located in seemingly normal brain parenchyma close to MRI-defined abnormalities, the second one in areas of FLAIR-defined abnormalities, the third one in areas of contrast enhancement when present, and the fourth one in areas of necrosis when present. Each biopsy sample was sent individually to neuropathology after marking spatial orientation according to MRI-defined abnormalities. Intraoperative histomolecular frozen analyses were performed, at the neurosurgeon's discretion, on the first set of serial biopsies to guide the biopsy procedure and perform, if required, a second series of biopsy sampling. Postoperative imaging (computed tomography or MRI) was planned on postoperative day 1.

End Points

The diagnostic yield of the stereotactic biopsy procedure was defined as a positive histomolecular diagnosis allowing for a dedicated oncologic treatment to be decided.

The safety of the stereotactic biopsy procedure was defined as the biopsy-related morbidity. We analyzed the prevalence and risk factors of new postoperative neurologic deficit, postoperative disability (defined as a Karnofsky Performance Status [KPS] decrease $\geq$20 points in the immediate postoperative period in relation to preoperative KPS score), bleeding at biopsy site on postoperative imaging, increased mass effect on postoperative imaging, discharge disposition (home or institution), and death within the first postoperative month.

Statistical Analyses

Continuous variables were described as mean $\pm$ standard deviation. Categorical variables were described as percentages. Univariable analyses were carried out, computing unadjusted odds ratios and using the χ^2 or Fisher exact test for comparing categorical variables, and the unpaired t test or Mann-Whitney U test for continuous variables, as appropriate. Variables associated at the $P < 0.05$ level in unadjusted analysis were entered into logistic regression models. We performed a backward stepwise selection of variables, removing the least significant variables one after the other, and defining the least significant variable as having the highest P value in the model. The final model retained only the variables significant at the $P < 0.05$ level. Statistical analyses were performed using JMP software version 14.1.0 (SAS Institute Inc., Cary, North Carolina, USA).

RESULTS

Population

A total of 377 patients (60.5% men; mean age, 59.9 $\pm$ 14.0 years) were included. Clinical and imaging characteristics are detailed in Table 1 and Figure 2.

Stereotactic Biopsy Procedure

Intraoperative characteristics are detailed in Table 2. There were no technical failures leading to biopsy arrest. A mean of 4.2 $\pm$ 1.9 (range, 1–14) biopsy samples were obtained at a mean of 2.6 $\pm$ 1.2 (range, 1–6) biopsy sites. Intraoperative bleeding through the biopsy cannula was observed in 27 patients (7.2%) after a mean of 4.3 $\pm$ 1.7 biopsy samples (range, 1–8) and led to sampling arrest in 13 patients (48.1%).

Serial biopsy sampling was performed at various sites encompassing the different components of MRI-defined abnormalities: a mean of 1.5 $\pm$ 1.2 (range, 0–7) samples in areas of contrast enhancement, and a mean of 1.0 $\pm$ 1.1 (range, 0–6) samples in areas of hyperintensity on FLAIR sequence. The histopathologic informativity of the biopsy samples varied with their location according to the components of MRI-defined abnormalities: 524/561 (93.4%) in the contrast-enhanced areas, 287/335 (85.7%) in the FLAIR hyperintense areas, 21/27 (77.8%) in the necrotic areas, 14/19 (73.7%) in the cystic areas, and 22/37 (59.5%) in the apparently normal brain parenchyma.

A histopathologic frozen analysis was performed intraoperatively in 324 patients (85.9%) in the first set of biopsy sampling. It was not performed in 53 patients (14.1%) presenting with a ringlike pattern of contrast enhancement with central necrosis on preoperative MRI because of the neurosurgeon's observation of the intraoperative macroscopic tumor appearance being concordant with the imaging characteristics for each biopsy sampling site (solid tumor tissue when sampling within the areas of contrast enhancement, necrosis when sampling within the central necrosis) in 49 patients (13.0%) and because of an intraoperative bleeding event precluding further biopsy samples from being obtained in the remaining 4 patients (1.1%). When performed, the intraoperative histopathologic frozen analysis guided the biopsy sampling procedure in 315 patients (97.2%), ending sampling because there were enough and informative biopsy samples in 270 patients and because of a need for a second set of biopsy samples in 45 patients. The analysis did not influence the surgical procedure in the remaining 9 patients (2.8%) because intraoperative bleeding precluding further biopsy samples from being obtained.

Diagnostic Yield of the Stereotactic Biopsy Procedure

The histomolecular diagnosis according to the cIMPACT-NOW (Consortium to Inform Molecular and Practical Approaches to CNS Tumor Taxonomy) updates in the WHO 2016 Classifications of Tumors of the Central Nervous System is detailed in Table 2.[1,2] The histomolecular diagnosis of a diffuse glioma and the glioma grade were obtained in 98.7% and in 92.6% of patients, respectively. In the 5 inconclusive cases (1.3%), the diagnosis was confirmed during a second surgical procedure. No predictor of a positive histomolecular diagnosis was identified, whereas male sex and a ringlike pattern of contrast enhancement with central necrosis on MRI were independent predictors of conclusive diffuse glioma grading (Table 3). The histomolecular diagnosis of a diffuse glioma and the glioma grade prediction rates varied according to the results of intraoperative histopathologic frozen analysis: 100% and 100%, respectively, when not performed because of the observation of a macroscopic tumor appearance; 100% and 85.7%, respectively, when not performed because of an intraoperative bleeding

Table 1. Patient and Tumor Characteristics at Diagnosis (n = 377)

Parameters	Value
Sex	
Male	228 (60.5)
Female	149 (39.5)
Age (years), median, mean ± SD, range	63, 59.9 ± 14.0, 18–86
<60 years	159 (42.2)
≥60 years	218 (57.8)
Arterial hypertension	
No	235 (62.3)
Yes	142 (37.7)
Anticoagulant therapy	
No	345 (91.5)
Yes	32 (8.5)
Preventive	10
Curative	22
Antiplatelet therapy	
No	329 (87.3)
Yes	48 (12.7)
Epileptic seizures	
No	218 (57.8)
Yes	159 (42.2)
Increased intracranial pressure	
No	298 (79.0)
Yes	70 (21.1)
Neurologic and/or cognitive deficit	
No	106 (28.1)
Yes	271 (71.9)
Karnofsky Performance Status (median, mean ± SD, range)	80, 77 ± 17, 20–100
<70	74 (16.6)
≥70	303 (80.4)
Main location of the lesion	
Frontal	153 (40.6)
Temporal	65 (17.2)
Parietal	80 (21.3)
Insular	16 (4.2)
Occipital	6 (1.6)
Cingular	6 (1.6)
Deep gray nuclei	51 (13.5)
Side of the lesion	
Left	156 (41.4)
Right	112 (29.7)
Bilateral	109 (28.9)
Contrast enhancement	
None	39 (10.4)
Faint and patchy	45 (11.9)
Nodular	54 (14.3)
Ringlike with central necrosis	239 (63.4)
Mass effect on midline	
No	207 (54.9)
Yes	161 (42.7)
Missing	9 (2.4)
Cortical infiltration	
No	113 (30.0)
Yes	254 (67.4)
Missing	10 (2.6)
Subventricular zone contact	
No	149 (39.5)
Yes	217 (57.6)
Missing	11 (2.9)
Volume of the contrast-enhanced area (cm^3), median, mean ± SD, range*	13.0, 22.4 ± 29.0, 0.1–184.4
Volume of the fluid-attenuated inversion recovery abnormalities (cm^3), median, mean ± SD, range	58.3, 75.2 ± 62.1, 3.2–305.4

Values are number (%) except where indicated otherwise.
SD, standard deviation.
*Of the contrast-enhanced area for the 338 patients with a contrast-enhancing tumor.

event; 100% and 92.8%, respectively, when intraoperative histopathologic frozen analysis concluded to the end of sampling because there were enough and informative biopsy samples; and 91.5% and 80.0%, respectively, when intraoperative histopathologic frozen analysis concluded the need for a second set of biopsy samples ($P = 0.045$).

Twenty-one patients under study (5.6%) benefited from 2 histopathologic analyses of 2 different samples: the first sample was obtained and analyzed as a result of the present stereotactic procedure, and the second one as a result of subsequent surgical removal of the glioma. The mean delay between both surgeries was 14.9 ± 21.1 months (range, 0.5–64 months). In the 11 patients with available comparisons, the 2 surgeries were performed before any oncologic treatments at a mean of 2.2 ± 2.9 months (range, 0.5–8 months), and histomolecular analyses were comparable in all cases (100%).

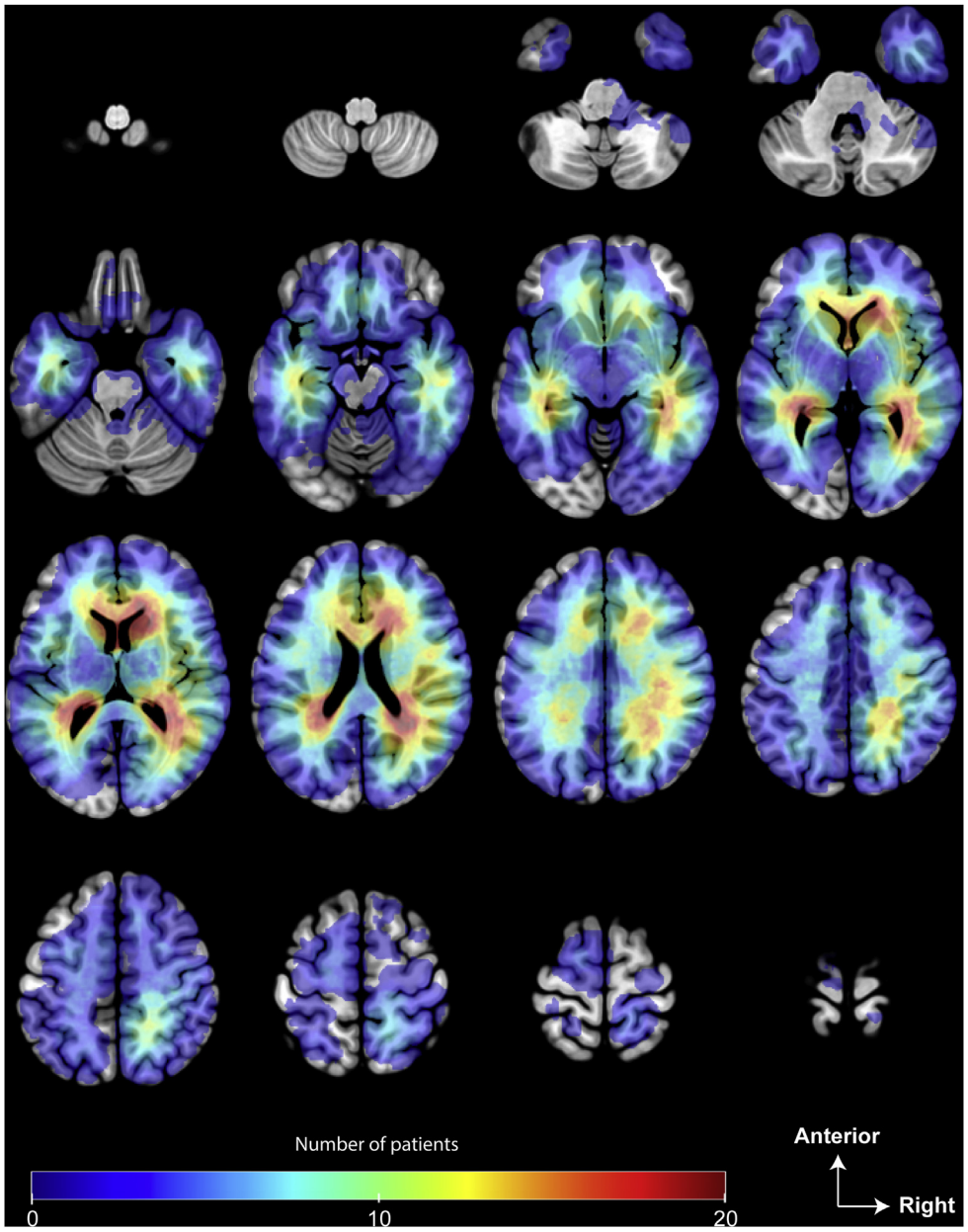

Figure 2. Location and frequency of patients with diffuse glioma included in the present study ($n = 377$). The color frequency map shows the location of patients with diffuse glioma. Images are shown in neurologic display convention.

Morbidity Related to the Stereotactic Biopsy Procedure

Postoperative characteristics are detailed in Table 2. Postoperative clinical complications included transient and permanent new neurologic deficit in 7.7%, epileptic seizures in 2.7%, systemic thromboembolic events in 1.3%, and intracerebral hematoma requiring surgical evacuation in 0.8%. No infection was observed. A KPS decrease of $\geq$20 points postoperatively (defining postoperative disability) was observed in 4.0%. Eleven patients (2.9%) died within the first postoperative month, and 4 (1.1%) died during their hospital stay. These deaths were directly related to tumor progression (altered KPS and therapeutic abstention) and not related to postoperative

Table 2. Intraoperative and Postoperative Characteristics (N = 377)

Intraoperative Characteristics	Value
Steroid use at the time of surgery	
No	137 (40.5)
Yes	201 (59.5)
Number of biopsy samples (median, mean ± SD, range)	4, 4.2 ± 1.9, 1–14
<4	148 (39.3)
4	87 (23.1)
≥4	142 (37.7)
Intraoperative hemorrhage	
No	350 (92.8)
Yes	27 (7.2)
Intraoperative histopathologic frozen analysis	
No	53 (14.1)
Neurosurgeon's convenience	49
Aborted because of intraoperative hemorrhage	4
Yes	324 (85.9)
Informative: sufficient material obtained	270
Informative: additional sampling required	45
Enough material after additional sampling	40
Inconclusive despite additional sampling	5
Limited by intraoperative hemorrhage	9
World Health Organization 2016 Classification of Central Nervous System Tumors + cIMPACT-NOW	
Diffuse astrocytoma, grade II, IDH-mutant	6 (1.6)
Diffuse astrocytoma, grade II, IDH-wildtype	1 (0.3)
Anaplastic diffuse astrocytoma, grade III, IDH-mutant	12 (3.2)
Anaplastic diffuse astrocytoma, grade III, IDH-wildtype	4 (1.1)
Anaplastic diffuse astrocytoma, grade III, NOS	4 (1.1)
Oligodendroglioma, grade II, IDH-mutant and 1p/19q-codeleted	14 (3.7)
Anaplastic oligodendroglioma, grade III, IDH-mutant and 1p/19q-codeleted	10 (2.7)
Glioblastoma, IDH-mutant	4 (1.1)
Glioblastoma, IDH-wildtype	265 (70.3)
Epithelioid glioblastoma, IDH-wildtype	2 (0.5)
Glioblastoma, NOS	11 (2.9)
Diffuse midline glioma, H3K27M-mutant	2 (0.5)
Diffuse astrocytic glioma, IDH-wildtype, with molecular features of glioblastoma	14 (3.7)
Diffuse glioma, NOS	23 (6.1)

Continues

Table 2. Continued

Intraoperative Characteristics	Value
Inconclusive	5 (1.3)
Clinical postoperative characteristics	
Karnofsky Performance Status (median, mean ± SD, range)	80, 76.0 ± 19.3, 10–100
<70	85 (22.5)
≥70	292 (77.5)
Karnofsky Performance Status decrease ≥20 points after surgery	
No	15 (4.0)
Yes	362 (96.0)
Epileptic seizures	
No	367 (97.3)
Yes	10 (2.7)
Postoperative neurologic deficit	
No	346 (92.3)
Yes	29 (7.7)
Hematoma requiring surgical evacuation	
No	374 (99.2)
Yes	3 (0.8)
Systemic thromboembolic event	
No	372 (98.7)
Yes	5 (1.3)
Length of hospital stay (days), median, mean ± SD, range	5, 7.6 ± 8.9, 2–111
Mode of discharge	
Home	235 (63.0)
Another institution	138 (37.0)
Imaging postoperative characteristics	
Bleeding at biopsy site (diameter)	
No	224 (59.4)
Yes	153 (40.6)
<5 mm	55
5–10 mm	43
10–20 mm	40
≥20 mm	15
Ischemia	
No	375 (99.5)
Yes	2 (0.5)
Increased mass effect	
No	364 (96.6)
Yes	13 (4.4)

Values are number (%) except where indicated otherwise.
SD, standard deviation; IDH, isocitrate dehydrogenase; NOS, not otherwise specified.

Table 3. Independent Risk Factors of Positive World Health Organization Glioma Grading

		Unadjusted OR			Adjusted OR*		
Parameters		**OR**	**95% CI**	***P* Value**	**Adjusted OR**	**95% CI**	***P* Value**
Sex	Female	1 (ref)			1 (ref)		
	Male	3.19	1.44–7.06	**0.003**	3.23	1.43–7.25	**0.004**
Age	<60 years	1 (ref)					
	≥60 years	2.06	0.95–4.43	0.064			
Contrast enhancement	None	1 (ref)			1 (ref)		
	Faint and patchy	2.65	0.72–9.59	0.139	2.49	0.67–9.27	0.173
	Nodular	2.53	0.76–8.43	0.131	2.48	0.72–8.48	0.147
	Ringlike with central necrosis	4.89	1.85–12.88	**0.001**	4.92	1.82–13.24	**0.002**
Volume of the contrast-enhanced area	<13 cm^3	1 (ref)					
	≥13 cm^3	2.38	1.02–5.56	**0.036**			
Steroid use at the time of surgery	No	1 (ref)					
	Yes	2.12	0.94–4.77	0.066			
Number of biopsy samples	<4	1 (ref)					
	4	2.69	0.87–8.28	0.084			
	≥4	2.17	0.91–5.21	0.081			

OR, odds ratio; CI, confidence interval.
Bold p-values indicates statistically significant ones.
*Multivariable backward stepwise logistic regression model.

complications (no postoperative hematoma ≥10 mm). Postoperative imaging (372 computed tomography scans, 98.7%; 5 MRIs, 1.3%) was performed at day zero in 26.5%, at day 1 in 58.6%, and at day 2 or more from surgery in 14.9% (mean, 23.6 ± 16.9 postoperative hours; range, 1–120 hours). Postoperative imaging complications included bleeding at the biopsy site ≥10 mm in 14.6% (<20 mm in 10.6%, and ≥20 mm in 4.0%), increased mass effect in 4.4%, and cerebral ischemia in 0.5%.

In the multivariable analyses, a preoperative neurologic deficit ($P = 0.030$), bleeding at the biopsy site ≥20 mm on postoperative imaging ($P = 0.004$), and increased mass effect on postoperative imaging ($P = 0.014$) were independent predictors of a new postoperative neurologic deficit (Table 4). A postoperative neurologic deficit ($P < 0.001$) and increased mass effect on postoperative imaging ($P = 0.014$) were independent predictors of a KPS decrease of ≥20 points postoperatively (Table 4). No predictor of an intracerebral hematoma requiring surgical evacuation was identified. Only preoperative anticoagulant therapy (although systematically stopped preoperatively according to guidelines of the *Haute Autorité de Santé* [French National Health Agency]) ($P = 0.017$) was an independent predictor of bleeding at the biopsy site ≥20 mm on postoperative imaging (Table 4). Clinical signs of increased intracranial pressure preoperatively ($P = 0.048$) and volume of the contrast-enhanced area ≥13 cm^3 on preoperative MRI ($P = 0.048$) were independent predictors of increased mass effect on postoperative imaging (Table 4). The number of biopsy sites and the number of biopsy samples were not independent risk factors of new postoperative neurologic deficits, postoperative disability, bleeding at the biopsy site, and increased mass effect on postoperative imaging.

Postoperative Management

The median length of hospital stay was 2 days (25% quartile 2, 75% quartile 5). The mean length of hospital stay (7.62 ± 8.90 days; range, 0–111 days) was increased by 51 patients (13.5%) with a length of hospital stay >7 days. After the biopsy procedure, 63.0% of patients returned home and the remaining patients were discharged to another institution.

In the multivariable analyses, a preoperative neurologic deficit ($P = 0.005$), a preoperative KPS <70 ($P < 0.001$), subventricular zone contact ($P = 0.004$), a faint and patchy pattern of contrast enhancement ($P = 0.018$), a nodular pattern of contrast enhancement ($P = 0.033$), a ringlike with central necrosis pattern of contrast enhancement ($P = 0.021$), and steroid use at the time of surgery ($P = 0.003$) were independent predictors of the inability to discharge patients home postoperatively (Table 5). When stratifying the rate of the inability to discharge patients home postoperatively by the number of predictors present in a particular patient, the rate of discharge to home decreased as follows: 100%, 96.0%, 87.8%, 55.8%; 45.4%, and 20.0%, with the increase from 0 to 5 of the predictors identified above when present (Figure 3). The number of biopsy sites and the number

Table 4. Independent Risk Factors of Postoperative Complications

		Unadjusted OR			Adjusted OR*		
Parameters		**OR**	**95% CI**	***P* Value**	**Adjusted OR**	**95% CI**	***P* Value**
Increased mass effect on postoperative imaging							
Age	<60 years	1 (ref)					
	≥60 years	2.50	0.68–9.24	0.147			
Increased intracranial pressure at surgery	No	1 (ref)			1 (ref)		
	Yes	3.42	1.11–10.47	**0.038**	3.37	1.01–11.26	**0.048**
Volume of the contrast-enhanced area	<13 cm^3	1 (ref)			1 (ref)		
	≥13 cm^3	6.50	1.42–29.77	**0.004**	5.19	1.09–24.79	**0.039**
Intraoperative hemorrhage	No	1 (ref)					
	Yes	4.25	1.10–16.48	0.064			
Number of biopsy samples	<4	1 (ref)					
	≥4	0.29	0.06–1.33	0.072			
New neurologic deficit							
Arterial hypertension	No	1 (ref)					
	Yes	2.18	1.01–4.67	**0.046**			
Anticoagulant and/or antiplatelet therapy	No	1 (ref)					
	Yes	2.33	1.01–5.38	0.059			
Preoperative neurologic and/or cognitive deficit	No	1 (ref)			1 (ref)		
	Yes	3.67	1.09–12.41	**0.015**	4.01	1.15–14.04	**0.030**
Preoperative Karnofsky Performance Status	≥70	1 (ref)					
	<70	2.32	1.03–5.23	0.052			
Preoperative steroid use at the time of surgery	No	1 (ref)					
	Yes	2.17	0.83–5.62	0.093			
Final histopathologic grading	Yes	1 (ref)					
	No	3.67	1.36–9.89	**0.010**			
Hemorrhage on postoperative imaging (diameter, mm)	No	1 (ref)			1 (ref)		
	10–20	2.18	0.70–6.81	0.180	1.83	0.56–5.96	0.317
	≥20	5.89	1.70–20.36	**0.005**	7.05	1.84–27.12	**0.004**
Increased mass effect on postoperative imaging	No	1 (ref)			1 (ref)		
	Yes	5.99	1.72–20.83	**0.013**	5.35	1.41–20.30	**0.014**
Hemorrhage ≥20 mm on postoperative imaging							
Preoperative anticoagulant therapy	No	1 (ref)			1 (ref)		
	Yes	4.33	1.29–14.51	**0.017**	4.29	1.27–14.48	**0.019**
Increased intracranial pressure at surgery	No	1 (ref)					
	Yes	3.85	0.50–29.69	0.118			
Neoangiogenesis	No	1 (ref)					
	Yes	2.62	0.86–7.95	0.108			

Continues

Table 4. Continued

Parameters		Unadjusted OR			Adjusted OR*		
		OR	95% CI	*P* Value	Adjusted OR	95% CI	*P* Value
Postoperative Karnofsky Performance Status decrease ≥20 points							
Preoperative neurologic and/or cognitive deficit	No	1 (ref)					
	Yes	2.83	0.63–12.68	0.126			
Subventricular zone contact	No	1 (ref)					
	Yes	2.12	0.67–6.72	0.178			
Hemorrhage on postoperative imaging (diameter)	No	1 (ref)					
	10–20 mm	3.12	0.82–11.3	0.095			
	≥20 mm	4.48	0.90–22.29	0.067			
Postoperative neurologic deficit	No	1 (ref)			1 (ref)		
	Yes	29.82	9.80–90.73	**<0.001**	25.56	8.08–80.91	**<0.001**
Postoperative hematoma requiring surgical evacuation	No	1 (ref)					
	Yes	51.43	4.39–601.43	**0.002**			
Ischemia on postoperative imaging	No	1 (ref)					
	Yes	24.0	1.43–402.45	0.055			
Increased mass effect on postoperative imaging	No	1 (ref)			1 (ref)		
	Yes	13.04	3.51–48.36	**0.001**	8.02	1.51–42.49	**0.014**

OR, odds ratio; CI, confidence interval.
Bold p-values indicates statistically significant ones.
*Multivariable backward stepwise logistic regression model.

of biopsy samples were not independent risk factors for discharge disposition, nor was death within the first postoperative month.

DISCUSSION

Key Results

In this retrospective monocentric cohort study of MRI-based robot-assisted stereotactic serial biopsy sampling in 377 adult patients harboring a supratentorial diffuse glioma, we show that 1) multiple biopsy sites (mean, 2.6, up to 6) with multiple biopsy samples (mean, 4.2, up to 14) along a single biopsy trajectory are feasible with low complication rates; 2) the histopathologic diagnostic yield of the biopsy samples varied with their location according to the MRI-defined abnormalities, from >93% in the contrast-enhanced areas to <60% in the apparently normal brain parenchyma areas; 3) the histopathologic frozen analysis, when performed intraoperatively, informed the biopsy sampling procedure in 97.2% of cases; 4) the histomolecular diagnosis of a diffuse glioma was obtained in 98.7% of cases and a conclusive grading was obtained in 92.6% of cases; 5) preoperative neurologic deficit, preoperative KPS <70, subventricular zone contact, contrast enhancement, and steroid use were predictors of the inability to discharge to home postoperatively, occurring in 37.0% of cases; 6) preoperative KPS <70 and increased mass effect on postoperative imaging were predictors of death within 1 month from surgery, occurring in 2.9% of cases.

Interpretation

We report, to date, the largest cohort of MRI-based robot-assisted serial stereotactic biopsy sampling for diffuse supratentorial gliomas in adults.[10,11] The 4.0% rate of postoperative disability is comparable to frame-based or frameless stereotactic biopsy procedures.[15-17,25-43] The 7.7% rate of transient or permanent new neurologic deficit is related to nonsurgical gliomas with poorer prognosis.[27] Contrary to previous reports,[28,32,35,36] we did not identify deep-seated location as a predictor of postoperative complications, possibly because of the exclusion of brainstem gliomas.[44] Previous studies have identified multiple stereotactic biopsy trajectories, particularly for deep-seated lesions, and multiple biopsy attempts as risk factors of postoperative neurologic deficits.[16,35,38] Here, after multiple serial sampling along a unique biopsy trajectory, the number of biopsy sites and the number of biopsy samples did not increase complication rates. The high level of attention to surgical technique details may have minimized the morbidity. Regarding postoperative bleeding at the biopsy site, the systematic completion of postoperative imaging led to the identification of numerous silent hemorrhages, without any clinical significance. The 14.6% rate of postoperative bleeding at the biopsy site is comparable to

Table 5. Independent Risk Factors of Postoperative Management

Parameters		Unadjusted OR			Adjusted OR*		
		OR	95% CI	*P* Value	Adjusted OR	95% CI	*P* Value
Inability to discharge to home postoperatively							
Age (years)	<60	1 (ref)					
	≥60	1.70	1.10–2.63	**0.015**			
Arterial hypertension	No	1 (ref)					
	Yes	1.69	1.10–2.60	**0.017**			
Anticoagulant and/or antiplatelet therapy	No	1 (ref)					
	Yes	1.92	1.12–3.29	**0.017**			
Increased intracranial pressure at surgery	No	1 (ref)					
	Yes	1.46	0.88–2.43	0.147			
Preoperative neurologic and/or cognitive deficit	No	1 (ref)			1 (ref)		
	Yes	5.59	3.04–10.31	**<0.001**	2.85	1.36–5.90	**0.005**
Preoperative Karnofsky Performance Status	≥70	1 (ref)			1 (ref)		
	<70	5.79	3.28–10.21	**<0.001**	4.01	2.06–7.81	**<0.001**
Volume of the contrast-enhanced area	<13 cm^3	1 (ref)					
	≥13 cm^3	3.71	2.35–5.85	**<0.001**			
Subventricular zone contact	No	1 (ref)			1 (ref)		
	Yes	3.58	2.21–5.79	**<0.001**	2.56	1.35–4.85	**0.004**
Contrast enhancement	None	1 (ref)			1 (ref)		
	Faint and patchy	5.44	1.12–26.63	**0.036**	14.22	1.57–128.83	**0.018**
	Nodular	7.12	1.52–33.27	**0.013**	10.35	1.20–89.02	**0.033**
	Ringlike with central necrosis	16.43	3.87–69.73	**<0.001**	11.28	1.45–87.68	**0.021**
Steroid use at the time of surgery	No	1 (ref)			1 (ref)		
	Yes	3.40	2.07–5.59	**<0.001**	2.20	1.18–4.12	**0.013**
Histopathologic diagnosis of glioblastoma	Yes	1 (ref)					
	No	0.37	0.22–0.61	**<0.001**			
Postoperative neurologic deficit	No	1 (ref)			1 (ref)		
	Yes	11.45	3.87–33.89	**<0.001**	7.44	1.99–27.86	**0.003**
Postoperative Karnofsky Performance Status decrease ≥20 points	No	1 (ref)					
	Yes	6.69	1.83–24.45	**0.001**			
Death during the first postoperative month							
Age (years)	<60	1 (ref)					
	≥60	3.38	0.72–15.86	0.085			
Increased intracranial pressure at surgery	No	1 (ref)					
	Yes	3.29	0.98–11.07	0.065			
Preoperative neurologic and/or cognitive deficit	No	1 (ref)					
	Yes	4.02	0.51–31.82	0.114			

Continues

Table 5. Continued

Parameters		Unadjusted OR			Adjusted OR*		
		OR	95% CI	*P* Value	Adjusted OR	95% CI	*P* Value
Preoperative Karnofsky Performance Status	≥70	1 (ref)			1 (ref)		
	<70	3.59	1.06–12.09	**0.049**	5.15	1.03–25.73	**0.045**
Volume of the contrast-enhanced area	<13 cm^3	1 (ref)					
	≥13 cm^3	5.25	1.12–24.67	**0.016**			
Postoperative neurologic deficit	No	1 (ref)					
	Yes	4.87	1.22–19.48	**0.047**			
Postoperative Karnofsky Performance Status decrease ≥20 points	No	1 (ref)					
	Yes	5.58	1.10–28.31	0.076			
Increased mass effect on postoperative imaging	No	1 (ref)			1 (ref)		
	Yes	22.67	5.62–91.48	**<0.001**	15.15	3.59–63.87	**<0.001**

OR, odds ratio; CI, confidence interval.
Bold p-values indicates statistically significant ones.
*Multivariable backward stepwise logistic regression model.

those observed in the context of glioma biopsies, ranging up to 53.9%.[45-47]

Previous studies have shown that increasing the number of biopsy samples of astrocytomas and targeting the different glioma components as observed on preoperative imaging may improve diagnostic accuracy.[22,40,48-50] We report one of the best diagnostic yield rates in the literature, ranging from 89% to 99.2%.[15,16,30,32,35-42,51,52] In addition, we observed a 100% concordance between histomolecular analyses performed on the first stereotactic biopsy and on the subsequent surgical resection sample in the 11 patients with available comparisons, which underlines the accuracy and the representativity of the stereotactic biopsy sampling method. This diagnostic consistency is higher than those reported in previous studies, ranging from 26% to 97%.[5,32,53,54] Muragaki et al.,[5] who performed only 1 biopsy sample in 66% of cases, showed a trend between the risk of undergrading and the low number of biopsy samples. The present results support the surgical strategy of multiple serial biopsy samples and sites, based on preoperative MRI and intraoperative histopathologic analyses when deemed informative, to maximize the diagnostic yield of stereotactic biopsy for diffuse gliomas in adults in the era of the WHO 2016 classification. The ongoing evolution of integrated histomolecular testing and of MRI radiomics features is leading to new diagnostic and prognostic markers using preoperative MRI and a limited amount of tissue, which may reduce the need for serial biopsy sampling for glioma diagnosis in the future.

There is a difficult balance between the possibility of outpatient care for most patients undergoing stereotactic biopsy and the rare but significant postoperative complications.[45,55-57] The identification of predictors of the inability to discharge to home postoperatively will help guide care of patients in daily practice. Inpatient care should be considered for patients predicted to not be discharged home postoperatively. The length of hospital stay was >7 days in 13.5% of cases because of the practical difficulties with patient discharge, often requiring a transfer to inpatient physical and rehabilitation medicine departments.[58]

Generalizability

In previous studies, different brain neoplasms, use of varying surgical techniques, and previous oncologic treatments affected the complication and diagnostic yield rates.[9,16,41,43,59] The present study controlled for this bias by selecting a homogeneous population. In addition, neuropathology interpretation bias was limited by the reassessment of all diffuse gliomas under study according to the 2016 updated WHO classification.[1,2] The

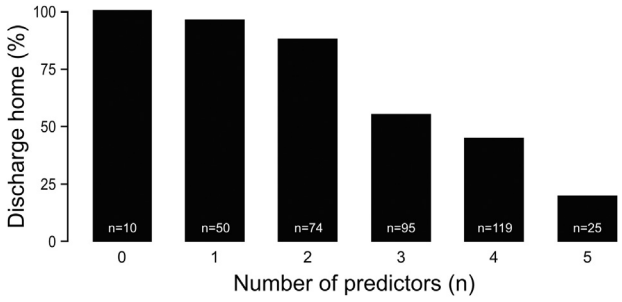

Figure 3. Stratification of the rate of inability to discharge to home by the number of predictors present in a particular patient: preoperative neurologic deficit, preoperative Karnofsky Performance Status <70, subventricular zone contact, contrast enhancement, and steroid use.

present study could help 1) envision multiple biopsy sites and samples encompassing all tumor components on MRI, allowing for histopathologic and molecular analyzes and storage without increasing complications rates; 2) identify cases at risk of tumor progression postoperatively; and 3) consider multiple robot-assisted MRI-based serial stereotactic biopsies as a safe and efficient diagnostic procedure.

Limitations

These findings should be interpreted with caution, given the retrospective and monocentric design, the exploratory design of statistical analyses, the lack of control group (conventional stereotactic procedures), and the lack of an external validation set, all limiting the generalizability of the results, and given the number of observed events that limited the number of predictive variables to be entered in multivariable models. Further confirmatory analyses are required to reproduce the present results.

CONCLUSIONS

Robot-assisted MRI-based multiple serial stereotactic biopsies for diffuse gliomas in adults is a safe and efficient procedure. Multiple biopsy sites, guided by MRI-defined abnormalities, and multiple biopsy samples, guided by intraoperative histopathologic frozen analysis, do not increase postoperative complication rates.

CRediT AUTHORSHIP CONTRIBUTION STATEMENT

Marc Zanello: Investigation, Data curation, Writing - original draft, Writing - review & editing. **Alexandre Roux:** Methodology, Investigation, Data curation, Writing - review & editing, Visualization. **Suhan Senova:** Investigation, Data curation, Writing - original draft, Writing - review & editing. **Sophie Peeters:** Writing - review & editing. **Myriam Edjlali:** Investigation, Writing - review & editing. **Arnault Tauziede-Espariat:** Investigation, Resources, Writing - review & editing. **Edouard Dezamis:** Investigation, Writing - review & editing. **Eduardo Parraga:** Investigation, Writing - review & editing. **Gilles Zah-Bi:** Investigation, Writing - review & editing. **Marc Harislur:** Investigation, Writing - review & editing. **Catherine Oppenheim:** Resources, Writing - review & editing. **Xavier Sauvageon:** Writing - review & editing. **Fabrice Chretien:** Resources, Writing - review & editing. **Bertrand Devaux:** Writing - review & editing. **Pascale Varlet:** Resources, Writing - review & editing. **Johan Pallud:** Conceptualization, Methodology, Formal analysis, Data curation, Writing - original draft, Writing - review & editing, Visualization, Supervision.

REFERENCES

1. Louis DN, Perry A, Reifenberger G, et al. The 2016 World Health Organization Classification of Tumors of the Central Nervous System: a summary. *Acta Neuropathol (Berl)*. 2016;131:803-820.
2. Brat DJ, Aldape K, Colman H, et al. cIMPACT-NOW update 3: recommended diagnostic criteria for "Diffuse astrocytic glioma, IDH-wildtype, with molecular features of glioblastoma, WHO grade IV." *Acta Neuropathol (Berl)*. 2018;136:805-810.
3. Ricard D, Idbaih A, Ducray F, Lahutte M, Hoang-Xuan K, Delattre J-Y. Primary brain tumours in adults. *Lancet*. 2012;379:1984-1996.
4. Müller MB, Schmidt MC, Schmidt O, et al. Molecular genetic analysis as a tool for evaluating stereotactic biopsies of glioma specimens. *J Neuropathol Exp Neurol*. 1999;58:40-45.
5. Muragaki Y, Chernov M, Maruyama T, et al. Low-grade glioma on stereotactic biopsy: how often is the diagnosis accurate? *Minim Invasive Neurosurg*. 2008;51:275-279.
6. Eigenbrod S, Trabold R, Brucker D, et al. Molecular stereotactic biopsy technique improves diagnostic accuracy and enables personalized treatment strategies in glioma patients. *Acta Neurochir (Wien)*. 2014;156:1427-1440.
7. Parker NR, Khong P, Parkinson JF, Howell VM, Wheeler HR. Molecular heterogeneity in glioblastoma: potential clinical implications. *Front Oncol*. 2015;5:55.
8. Beuvon F, Varlet P, Fallet-Bianco C, Daumas-Duport C. [The "smears" technique for the extemporaneous examination: diagnostic contribution to neurosurgical pathology]. *Ann Pathol*. 2000;20:499-506 [in French].
9. Lefranc M, Capel C, Pruvot-Occean A-S, et al. Frameless robotic stereotactic biopsies: a consecutive series of 100 cases. *J Neurosurg*. 2015;122:342-352.
10. Marcus HJ, VakhariaVN, Ourselin S, Duncan J, Tisdall M, Aquilina K. Robot-assisted stereotactic brain biopsy: systematic review and bibliometric analysis. *Childs Nerv Syst*. 2018;34:1299-1309.
11. Yasin H, Hoff H-J, Blümcke I, Simon M. Experience with 102 frameless stereotactic biopsies using the Neuromate robotic device. *World Neurosurg*. 2019;123:e450-e456.
12. Benabid AL, Hoffmann D, Ashraf A, Koudsie A, Esteve F, Le Bas J. La robotisation de la neurochirurgie: état actuel et perspectives d'avenir. *Chir Memoires Acad Chir*. 1998;123:25-31 [in French].
13. Fomenko A, Serletis D. Robotic stereotaxy in cranial neurosurgery: a qualitative systematic review. *Neurosurgery*. 2018;83:642-650.
14. Legnani FG, Franzini A, Mattei L, et al. Image-guided biopsy of intracranial lesions with a small robotic device (iSYS1): a prospective, exploratory pilot study. *Oper Neurosurg*. 2019;17:403-412.
15. Apuzzo ML, Chandrasoma PT, Cohen D, Zee CS, Zelman V. Computed imaging stereotaxy: experience and perspective related to 500 procedures applied to brain masses. *Neurosurgery*. 1987;20:930-937.
16. Hall WA. The safety and efficacy of stereotactic biopsy for intracranial lesions. *Cancer*. 1998;82:1749-1755.
17. Ferreira MP, Ferreira NP, Pereira Filho A de A, Pereira Filho G de A, Franciscatto AC. Stereotactic computed tomography-guided brain biopsy: diagnostic yield based on a series of 170 patients. *Surg Neurol*. 2006;65(suppl 1):S1:27-S1:32.
18. Ersahin M, Karaaslan N, Gurbuz MS, et al. The safety and diagnostic value of frame-based and CT-guided stereotactic brain biopsy technique. *Turk Neurosurg*. 2011;21:582-590.
19. Daumas-Duport C, Szikla G. [Definition of limits and 3D configuration of cerebral gliomas. Histological data, therapeutic incidences (author's transl)]. *Neurochirurgie*. 1981;27:273-284 [in French].
20. Kelly PJ, Daumas-Duport C, Kispert DB, Kall BA, Scheithauer BW, Illig JJ. Imaging-based stereotaxic serial biopsies in untreated intracranial glial neoplasms. *J Neurosurg*. 1987;66:865-874.
21. Daumas-Duport C, Monsaigneon V, Blond S, et al. Serial stereotactic biopsies and CT scan in gliomas: correlative study in 100 astrocytomas, oligoastrocytomas and oligodendrocytomas. *J Neurooncol*. 1987;4:317-328.
22. Pallud J, Varlet P, Devaux B, et al. Diffuse low-grade oligodendrogliomas extend beyond MRI-defined abnormalities. *Neurology*. 2010;74:1724-1731.
23. von Elm E, Altman DG, Egger M, et al. The Strengthening the Reporting of Observational Studies in Epidemiology (STROBE) statement: guidelines for reporting observational studies. *PLoS Med*. 2007;4:e296.
24. Daumas-Duport C, Meder JF, Monsaingeon V, Missir O, Aubin ML, Szikla G. Cerebral gliomas: malignancy, limits and spatial configuration.

Comparative data from serial stereotaxic biopsies and computed tomography (a preliminary study based on 50 cases). *J Neuroradiol*. 1983;10:51-80 [in French].

25. Bernstein M, Parrent AG. Complications of CT-guided stereotactic biopsy of intra-axial brain lesions. *J Neurosurg*. 1994;81:165-168.

26. Chen C-C, Hsu P-W, Erich Wu T-W, et al. Stereotactic brain biopsy: single center retrospective analysis of complications. *Clin Neurol Neurosurg*. 2009;111:835-839.

27. Dhawan S, He Y, Bartek J, Alattar AA, Chen CC. Comparison of frame-based versus frameless intracranial stereotactic biopsy: systematic review and meta-analysis. *World Neurosurg*. 2019;127:607-616.e4.

28. Field M, Witham TF, Flickinger JC, Kondziolka D, Lunsford LD. Comprehensive assessment of hemorrhage risks and outcomes after stereotactic brain biopsy. *J Neurosurg*. 2001;94:545-551.

29. Hamisch CA, Minartz J, Blau T, et al. Frame-based stereotactic biopsy of deep-seated and midline structures in 511 procedures: feasibility, risk profile, and diagnostic yield. *Acta Neurochir (Wien)*. 2019;161:2065-2071.

30. Heper AO, Erden E, Savas A, et al. An analysis of stereotactic biopsy of brain tumors and nonneoplastic lesions: a prospective clinicopathologic study. *Surg Neurol*. 2005;64(suppl 2):S82-S88.

31. Kellermann SG, Hamisch CA, Rueß D, et al. Stereotactic biopsy in elderly patients: risk assessment and impact on treatment decision. *J Neurooncol*. 2017;134:303-307.

32. Kim JE, Kim DG, Paek SH, Jung H-W. Stereotactic biopsy for intracranial lesions: reliability and its impact on the planning of treatment. *Acta Neurochir (Wien)*. 2003;145:547-554 [discussion 554-555].

33. Kondziolka D, Firlik AD, Lunsford LD. Complications of stereotactic brain surgery. *Neurol Clin*. 1998;16:35-54.

34. Krieger MD, Chandrasoma PT, Zee CS, Apuzzo ML. Role of stereotactic biopsy in the diagnosis and management of brain tumors. *Semin Surg Oncol*. 1998;14:13-25.

35. McGirt MJ, Woodworth GF, Coon AL, et al. Independent predictors of morbidity after image-guided stereotactic brain biopsy: a risk assessment of 270 cases. *J Neurosurg*. 2005;102:897-901.

36. Owen CM, Linskey ME. Frame-based stereotaxy in a frameless era: current capabilities, relative role, and the positive- and negative predictive values of blood through the needle. *J Neurooncol*. 2009;93:139-149.

37. Paleologos TS, Dorward NL, Wadley JP, Thomas DG. Clinical validation of true frameless stereotactic biopsy: analysis of the first 125 consecutive cases. *Neurosurgery*. 2001;49:830-835 [discussion 835-837].

38. Sawin PD, Hitchon PW, Follett KA, Torner JC. Computed imaging-assisted stereotactic brain biopsy: a risk analysis of 225 consecutive cases. *Surg Neurol*. 1998;49:640-649.

39. Tilgner J, Herr M, Ostertag C, Volk B. Validation of intraoperative diagnoses using smear preparations from stereotactic brain biopsies: intraoperative versus final diagnosis—influence of clinical factors. *Neurosurgery*. 2005;56:257-265 [discussion 257-265].

40. Ulm AJ, Bova FJ, Friedman WA. Stereotactic biopsy aided by a computer graphics workstation: experience with 200 consecutive cases. *Surg Neurol*. 2001;56:366-371 [discussion 371-372].

41. Woodworth GF, McGirt MJ, Samdani A, Garonzik I, Olivi A, Weingart JD. Frameless image-guided stereotactic brain biopsy procedure: diagnostic yield, surgical morbidity, and comparison with the frame-based technique. *J Neurosurg*. 2006;104:233-237.

42. Yamada K, Goto S, Kochi M, Ushio Y. Stereotactic biopsy for multifocal, diffuse, and deep-seated brain tumors using Leksell's system. *J Clin Neurosci*. 2004;11:263-267.

43. Zhang Q-J, Wang W, Wei X, Yu Y. Safety and efficacy of frameless stereotactic brain biopsy techniques. *Chin Med Sci*. 2013;28:113-116.

44. Kickingereder P, Willeit P, Simon T, Ruge MI. Diagnostic value and safety of stereotactic biopsy for brainstem tumors: a systematic review and meta-analysis of 1480 cases. *Neurosurgery*. 2013;72:873-881 [discussion 882; quiz 882].

45. Kulkarni AV, Guha A, Lozano A, Bernstein M. Incidence of silent hemorrhage and delayed deterioration after stereotactic brain biopsy. *J Neurosurg*. 1998;89:31-35.

46. Kreth FW, Muacevic A, Medele R, Bise K, Meyer T, Reulen HJ. The risk of haemorrhage after image guided stereotactic biopsy of intra-axial brain tumours—a prospective study. *Acta Neurochir (Wien)*. 2001;143:539-545 [discussion 545-546].

47. Mizobuchi Y, Nakajima K, Fujihara T, et al. The risk of hemorrhage in stereotactic biopsy for brain tumors. *J Med Investig*. 2019;66:314-318.

48. Kondziolka D, Lunsford LD. The role of stereotactic biopsy in the management of gliomas. *J Neurooncol*. 1999;42:205-213.

49. McGirt MJ, Villavicencio AT, Bulsara KR, Friedman AH. MRI-guided stereotactic biopsy in the diagnosis of glioma: comparison of biopsy and surgical resection specimen. *Surg Neurol*. 2003;59:277-281 [discussion 281-282].

50. Daumas-Duport C, Varlet P, Tucker ML, Beuvon F, Cervera P, Chodkiewicz JP. Oligodendrogliomas. Part I: Patterns of growth, histological diagnosis, clinical and imaging correlations: a study of 153 cases. *J Neurooncol*. 1997;34:37-59.

51. O'Neill KS, Dyer PV, Bell BA, Wilkins PR, Uttley D, Marsh HT. Is peroperative smear cytology necessary for CT-guided stereotaxic biopsy? *Br J Neurosurg*. 1992;6:421-427.

52. Ranjan A, Rajshekhar V, Prakash GS, Joseph T, Chandy MJ, Chandi SM. CT guided stereotactic surgery: an overview of 600 procedures. *Neurol India*. 1993;41:193-197.

53. Woodworth G, McGirt MJ, Samdani A, Garonzik I, Olivi A, Weingart JD. Accuracy of frameless and frame-based image-guided stereotactic brain biopsy in the diagnosis of glioma: comparison of biopsy and open resection specimen. *Neurol Res*. 2005;27:358-362.

54. Jackson RJ, Fuller GN, Abi-Said D, et al. Limitations of stereotactic biopsy in the initial management of gliomas. *Neuro Oncol*. 2001;3:193-200.

55. Warnick RE, Longmore LM, Paul CA, Bode LA. Postoperative management of patients after stereotactic biopsy: results of a survey of the AANS/CNS section on tumors and a single institution study. *J Neurooncol*. 2003;62:289-296.

56. Bekelis K, Missios S, Roberts DW. Institutional charges and disparities in outpatient brain biopsies in four US States: the State Ambulatory Database (SASD). *J Neurooncol*. 2013;115:277-283.

57. Bhardwaj RD, Bernstein M. Prospective feasibility study of outpatient stereotactic brain lesion biopsy. *Neurosurgery*. 2002;51:358-361 [discussion 361-364].

58. Chevreul K, Brigham KB. Health system in France. In: van Ginneken E, Busse R, eds. *Health Care Systems and Policies. Health Services Research*. New York: Springer; 2018:1-10.

59. Terrier L, Gilard V, Marguet F, Fontanilles M, Derrey S. Stereotactic brain biopsy: evaluation of robot-assisted procedure in 60 patients. *Acta Neurochir (Wien)*. 2019;161:545-552.

Conflict of interest statement: The authors declare that the article content was composed in the absence of any commercial or financial relationships that could be construed as a potential conflict of interest.

Received 3 October 2020; accepted 26 December 2020

Citation: World Neurosurg. (2021) 148:e301-e313.
https://doi.org/10.1016/j.wneu.2020.12.127

Journal homepage: ***www.journals.elsevier.com/world-neurosurgery***

Available online: ***www.sciencedirect.com***

1878-8750/$ - see front matter